



Annales Geophysicae (ANGEO)

The Geminid meteor shower during the ECOMA sounding rocket campaign: specular and head echo radar observations

The ECOMA (Existence of Charge state Of meteoric smoke particles in the Middle Atmosphere) sounding rocket campaign was conducted during the Geminid meteor shower in December 2010 to explore whether there is a change of the properties of meteoric smoke particles due to the stream. The results are reported here.

Reference

Stober, G. et al.: [The Geminid meteor shower during the ECOMA sounding rocket campaign: specular and head echo radar observations](#), *Ann. Geophys.*, 31, 473-487, 2013



Geminid meteor over the Mojave Desert in 2009 (Credit: [Wally Pacholka, The World at Night](#))

Atmospheric Chemistry and Physics (ACP)

Recent variability of the solar spectral irradiance and its impact on climate modelling

Researchers summarise the current knowledge of solar spectral irradiance (SSI) variability and its impact on Earth's climate. They present a detailed overview of existing SSI measurements and provide thorough comparison of models available to date.

Reference

Ermolli, I. et al.: [Recent variability of the solar spectral irradiance and its impact on climate modelling](#), *Atmos. Chem. Phys.*, 13, 3945-3977, 2013

Oxidation of SO₂ by stabilized Criegee intermediate (sCI) radicals as a crucial source for atmospheric sulfuric acid concentrations

The effect of increased reaction rates of stabilised Criegee intermediates (sCIs) with SO₂ to produce sulfuric acid is investigated in this paper using data from two different locations, SMEAR II, Hyytiälä, Finland, and Hohenpeissenberg, Germany.

Reference

Boy, M. et al.: [Oxidation of SO₂ by stabilized Criegee intermediate \(sCI\) radicals as a crucial source for atmospheric sulfuric acid concentrations](#), *Atmos. Chem. Phys.*, 13, 3865-3879, 2013

Meteorological observations on the northern Chilean coast during VOCALS-REx

The authors report on surface coastal observations from two automatic weather stations at Pajopaso (~25° S) and radiosonde observations at Pajopaso and Iquique (~20° S) carried out during VOCALS-REx (VAMOS Ocean-Cloud-Atmosphere-Land Study Regional Experiment).

Reference

Rutllant, J. A., Muñoz, R. C., and Garreaud, R. D.: [Meteorological observations on the northern Chilean coast during VOCALS-REx](#), *Atmos. Chem. Phys.*, 13, 3409-3422, 2013

A unified approach to infrared aerosol remote sensing and type specification

In this paper, the researchers use high resolution infrared measurements for aerosol type differentiation, exploiting, in that part of spectrum, the dependency of their refractive index on wavelength. They review existing detection methods and present a unified detection method based on linear discrimination analysis.

Reference

Clarisse, L. et al.: [A unified approach to infrared aerosol remote sensing and type specification](#), *Atmos. Chem. Phys.*, 13, 2195-2221, 2013

Quantifying the uncertainty in simulating global tropospheric composition due to the variability in global emission estimates of Biogenic Volatile Organic Compounds

In this study researchers examine the contribution of biogenic volatile organic compounds towards global tropospheric composition using the global 3D chemistry transport model TM5 and the recently developed modified CB05 chemical mechanism.

Reference

Williams, J. E., van Velthoven, P. F. J. and Brenninkmeijer, C. A. M.: [Quantifying the uncertainty in simulating global tropospheric composition due to the variability in global emission estimates of Biogenic Volatile Organic Compounds](#), Atmos. Chem. Phys., 13, 2857-2891, 2013

Host model uncertainties in aerosol radiative forcing estimates: results from the AeroCom Prescribed intercomparison study

In this AeroCom Prescribed intercomparison study, researchers systematically isolate and quantify host model uncertainties on aerosol forcing experiments through prescription of identical aerosol radiative properties in twelve participating models.

Reference

Stier, P. et al.: [Host model uncertainties in aerosol radiative forcing estimates: results from the AeroCom Prescribed intercomparison study](#), Atmos. Chem. Phys., 13, 3245-3270, 2013

Atmospheric Measurement Techniques (AMT)

The CM SAF SSM/I-based total column water vapour climate data record: methods and evaluation against re-analyses and satellite

The European Organisation for the Exploitation of Meteorological Satellites (EUMETSAT) Satellite Application Facility on Climate Monitoring (CM SAF) aims at the provision and sound validation of well documented Climate Data Records (CDRs) in sustained and

operational environments. In this study, a total column water vapour path climatology from CM SAF is presented and inter-compared to water vapour data records from various data sources.

Reference

Schröder, M., et al.: [The CM SAF SSM/I-based total column water vapour climate data record: methods and evaluation against re-analyses and satellite](#), Atmos. Meas. Tech., 6, 765-775, 2013

Biogeosciences (BG)

Surface pathway of radioactive plume of TEPCO Fukushima NPP1 released ^{134}Cs and ^{137}Cs

^{134}Cs and ^{137}Cs were released to the North Pacific Ocean by two major likely pathways, direct discharge from the Fukushima Nuclear Power Plant 1 (NPP1) accident site and atmospheric deposition off Honshu Islands of Japan, east and northeast of the site. High density observations of ^{134}Cs and ^{137}Cs in the surface water were carried out by 17 cruises of cargo ships and several research vessel cruises from March 2011 until March 2012. The results are reported here.

Reference

Aoyama, M. et al.: [Surface pathway of radioactive plume of TEPCO Fukushima NPP1 released \$^{134}\text{Cs}\$ and \$^{137}\text{Cs}\$](#) , Biogeosciences, 10, 3067-3078, 2013

Bacteriohopanepolyols record stratification, nitrogen fixation and other biogeochemical perturbations in Holocene sediments of the central Baltic Sea

The team studied bacteriohopanepolyols, lipids of specific bacterial groups, in a sediment core from the central Baltic Sea (Gotland Deep) and found considerable differences between the distinct stages of the Baltic Sea's history.

Reference

Blumenberg, M. et al.: [Bacteriohopanepolyols record stratification, nitrogen fixation and other biogeochemical perturbations in Holocene sediments of the central Baltic Sea](#), Biogeosciences, 10, 2725-2735, 2013

Nitrous oxide emissions from European agriculture – an analysis of variability and drivers of emissions from field experiments

Nitrous oxide emissions from a network of agricultural experiments in Europe were used to explore the relative importance of site and management controls of emissions. At each site, a selection of management interventions were compared within replicated experimental designs in plot-based experiments.

Reference

Rees, R. M. et al.: [Nitrous oxide emissions from European agriculture – an analysis of variability and drivers of emissions from field experiments](#), *Biogeosciences*, 10, 2671-2682, 2013

Vertical distributions of plutonium isotopes in marine sediment cores off the Fukushima coast after the Fukushima Dai-ichi Nuclear Power Plant accident

To obtain the vertical distribution of Pu isotopes in marine sediments and to better assess the possible contamination of Pu from the Fukushima Dai-ichi Nuclear Power Plant accident in the marine environment, the researchers determined the activities of $^{239+240}\text{Pu}$ and ^{241}Pu as well as the atom ratios of $^{240}\text{Pu}/^{239}\text{Pu}$ and $^{241}\text{Pu}/^{239}\text{Pu}$ in sediment core samples collected in the western North Pacific off Fukushima from July 2011 to July 2012.

Reference

Bu, W. T. et al.: [Vertical distributions of plutonium isotopes in marine sediment cores off the Fukushima coast after the Fukushima Dai-ichi Nuclear Power Plant accident](#), *Biogeosciences*, 10, 2497-2511, 2013



The damaged Fukushima I Nuclear Power Plant after the 2011 Tohoku earthquake and tsunami. (Credit: Digital Globe)

Inverse estimation of source parameters of oceanic radioactivity dispersion models associated with the Fukushima accident

With combined use of the ocean–atmosphere simulation models and field observation data, we evaluate the parameters associated with the total caesium-137 amounts of the direct release into the ocean and atmospheric deposition over the western North Pacific caused by the accident of Fukushima Dai-ichi nuclear power plant that occurred in March 2011.

Reference

Miyazawa, Y. et al.: [Inverse estimation of source parameters of oceanic radioactivity dispersion models associated with the Fukushima accident](#), *Biogeosciences*, 10, 2349-2363, 2013

Short- and long-term consequences of larval stage exposure to constantly and ephemerally elevated carbon dioxide for marine bivalve populations

Experiments were performed to assess the short-term (days) and long-term (months) consequences of larval stage exposure to varying CO_2 concentrations for calcifying bivalves. The findings suggested that high CO_2 has a cascading negative physiological impact on bivalve larvae stemming in part from lower calcification rates.

Reference

Gobler, C. J. and Talmage, S. C.: [Short- and long-term consequences of larval stage exposure to constantly and ephemerally elevated carbon dioxide for marine bivalve populations](#), *Biogeosciences*, 10, 2241-2253, 2013

An unknown oxidative metabolism substantially contributes to soil CO_2 emissions

The respiratory release of CO_2 from soils is a major determinant of the global carbon cycle. It is traditionally considered that this respiration is an intracellular metabolism consisting of complex biochemical reactions carried out by numerous enzymes and co-factors. Here the researchers show that the endoenzymes released from dead organisms are stabilised in soils and have access to suitable substrates and co-factors to permit function.

Reference

Maire, V., et al.: [An unknown oxidative metabolism substantially contributes to soil \$\text{CO}_2\$ emissions](#), *Biogeosciences*, 10, 1155-1167, 2013

14 Open Access Journals
& newly launched:
Earth Surface Dynamics

The Cryosphere
Solid Earth
Ocean Science
Nonlinear Processes in Geophysics
Natural Hazards and Earth System Sciences
Hydrology and Earth System Sciences
Geoscientific Model Development
Geoscientific Instrumentation, Methods and Data Systems
Earth System Dynamics
Climate of the Past
Biogeosciences
Atmospheric Measurement Techniques
Atmospheric Chemistry and Physics
Annals of Geophysics

Climate of the Past (CP)

Direct linking of Greenland and Antarctic ice cores at the Toba eruption (74 ka BP)

In this work, the authors suggest a direct synchronisation of Greenland and Antarctic ice cores at the Toba eruption based on matching of a pattern of bipolar volcanic spikes. Annual layer counting between volcanic spikes in both cores allows for a unique match.

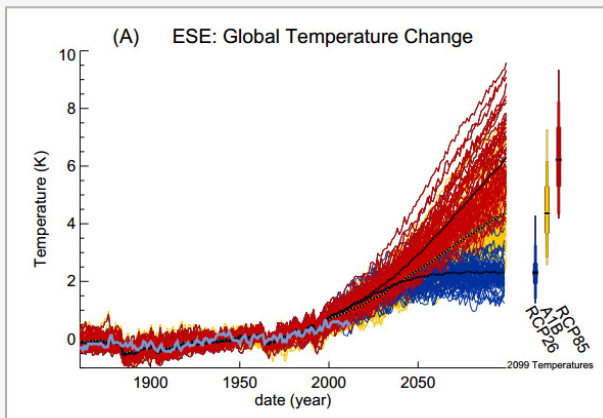
Reference

Svensson, A. et al.: [Direct linking of Greenland and Antarctic ice cores at the Toba eruption \(74 ka BP\)](#), *Clim. Past.*, 9, 749-766, 2013.



Lake and supervolcano Toba in Sumatra, Indonesia (Credit: NASA Landsat)

Earth System Dynamics (ESD)



The global mean temperature response to various climate scenarios (Credit: Booth et al., 2013)

Scenario and modelling uncertainty in global mean temperature change derived from emission-driven global climate models

In this work, the authors compare future changes in global mean temperature in response to different future scenarios which, for the first time, arise from emission-driven rather than concentration-driven perturbed parameter ensemble of a global climate model.

Reference

Booth, B. B. B. et al.: [Scenario and modelling uncertainty in global mean temperature change derived from emission-driven global climate models](#), *Earth Syst. Dynam.*, 4, 95-108, 2013

Geoscientific Instrumentation, Methods and Data Systems (GI)

Interpreting muon radiographic data in a fault zone: possible application to geothermal reservoir detection and monitoring

In this report, the data taken by Tanaka et al. (2011) are reanalysed to estimate the porosity distribution as a function of a distance from the fault gouge. The result shows a similar pattern of the porosity distribution as measured by borehole sampling at Nojima

fault. There is a low porosity shear zone axis surrounded by porous damaged areas with density increasing with the distance from the fault gouge. Applications of this work include drilling of geothermal exploration wells and geothermal exploration and monitoring.

Reference

Tanaka, H. K. M. and Muraoka, H.: [Interpreting muon radiographic data in a fault zone: possible application to geothermal reservoir detection and monitoring](#), *Geosci. Instrum. Method. Data Syst.*, 2, 145-150, 2013

Hydrology and Earth System Sciences (HESS)

Reducing cloud obscuration of MODIS snow cover area products by combining spatio-temporal techniques with a probability of snow approach

This study develops a rule-based, multistep method (including combining images from more than one satellite and other techniques) for removing clouds from MODIS snow cover area images.

Reference

López-Burgos, V., Gupta, H. V., and Clark, M.: [Reducing cloud obscuration of MODIS snow cover area products by combining spatio-temporal techniques with a probability of snow approach](#), Hydrol. Earth Syst. Sci., 17, 1809-1823, 2013

Elusive drought: uncertainty in observed trends and short- and long-term CMIP5 projections

The results presented here highlight the inherent difficulty of drought quantification and the considerable likelihood range of drought projections, but also indicate regions where drought is consistently found to increase.

Reference

Orlowsky, B. and Seneviratne, S. I.: [Elusive drought: uncertainty in observed trends and short- and long-term CMIP5 projections](#), Hydrol. Earth Syst. Sci., 17, 1765-1781, 2013

Comparative assessment of predictions in ungauged basins – Part 1: Runoff-hydrograph studies

The objective of this assessment is to compare studies predicting runoff hydrographs in ungauged catchments. The aim is to learn from the differences and similarities between catchments in different locations.

Reference

Parajka, J., et al.: [Comparative assessment of predictions in ungauged basins – Part 1: Runoff-hydrograph studies](#), Hydrol. Earth Syst. Sci., 17, 1783-1795, 2013

McMaster Mesonet soil moisture dataset: description and spatio-temporal variability analysis

This paper introduces and describes the hourly, high-resolution soil moisture dataset continuously recorded by the McMaster Mesonet located in the Hamilton-Halton Watershed in Ontario, Canada.

Reference

Kornelsen, K. C. and Coulibaly, P.: [McMaster Mesonet soil moisture dataset: description and spatio-temporal variability analysis](#), Hydrol. Earth Syst. Sci., 17, 1589-1606, 2013

Flood-initiating catchment conditions: a spatio-temporal analysis of large-scale soil moisture patterns in the Elbe River basin

Here, the authors propose classifying soil moisture as a key variable of pre-event catchment conditions and investigating the link between soil moisture patterns and flood occurrence in the Elbe River basin.

Reference

Nied, M., Hundecha, Y., and Merz, B.: [Flood-initiating catchment conditions: a spatio-temporal analysis of large-scale soil moisture patterns in the Elbe River basin](#), Hydrol. Earth Syst. Sci., 17, 1401-1414, 2013

Local and global perspectives on the virtual water trade

This paper presents and discusses the assessment of virtual water fluxes between a single country and its network of trading partners, delineating a country's virtual water budget in space and time (years 1986-2010).

Reference

Tamea, S., et al.: [Local and global perspectives on the virtual water trade](#), Hydrol. Earth Syst. Sci., 17, 1205-1215, 2013

A generalized Damköhler number for classifying material processing in hydrological systems

This paper focuses on the dynamic balance between transport and material transformation, and defines material connectivity as the effective transfer of material between elements of the hydrological cycle.

Reference

Oldham, C. E., Farrow, D. E., and Peiffer, S.: [A generalized Damköhler number for classifying material processing in hydrological systems](#), Hydrol. Earth Syst. Sci., 17, 1133-1148, 2013

A statistical analysis of insurance damage claims related to rainfall extremes

In this paper, a database of water-related insurance damage claims related to private properties and content is analysed. The aim is to investigate whether the probability of occurrence of rainfall-related damage is associated with the rainfall intensity.

Reference

Spekkers, M. H., et al.: [A statistical analysis of insurance damage claims related to rainfall extremes](#), Hydrol. Earth Syst. Sci., 17, 913-922, 2013

Natural Hazards and Earth System Sciences (NHESS)

Possible effects on avionics induced by terrestrial gamma-ray flashes

Terrestrial gamma-ray flashes (TGFs) are impulsive (intrinsically sub-millisecond) events associated with lightning in powerful thunderstorms. This article addresses the issue of the possible susceptibility of typical aircraft electronics exposed to TGF particle, gamma ray and neutron irradiation.

Reference

Tavani, M. et al.: [Possible effects on avionics induced by terrestrial gamma-ray flashes](#), Nat. Hazards Earth Syst. Sci., 13, 1127-1133, 2013

The influence of climate change on flood risks in France – first estimates and uncertainty analysis

This paper proposes a methodology to project the possible evolution of river flood damages due to climate change and applies it to mainland France.

Reference

Dumas, P., et al.: [The influence of climate change on flood risks in France – first estimates and uncertainty analysis](#), Nat. Hazards Earth Syst. Sci., 13, 809-821, 2013

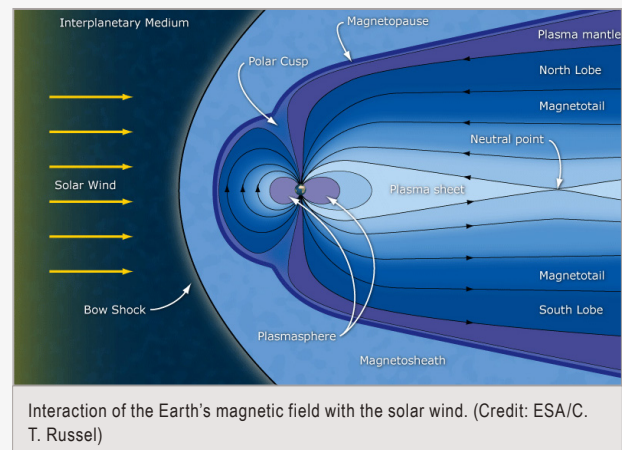
Nonlinear Processes in Geophysics (NPG)

Ion motion in the current sheet with sheared magnetic field – Part 1: Quasi-adiabatic theory

This paper presents a theory of trapped ion motion in the magnetotail current sheet with a constant dawn–dusk component of the magnetic field. Particle trajectories are described analytically using the quasi-adiabatic invariant corresponding to averaging of fast oscillations around the tangential component of the magnetic field.

Reference

Artemyev, A. V., Neishtadt, A. I., and Zelenyi, L. M.: [Ion motion in the current sheet with sheared magnetic field – Part 1: Quasi-adiabatic theory](#), Nonlin. Processes Geophys., 20, 163-178, 2013



Ocean Science (OS)



Areas where MERIS (MEDIum Resolution Imaging Spectrometer) data were extracted from ESA's MERCI, the MERIS Catalogue and Inventory, database. (Credit: Wernand et al., 2013)

MERIS-based ocean colour classification with the discrete Forel–Ule scale

Researchers present a new algorithm that uses the full spectral information in the visible domain to characterise natural waters in a simple and globally valid way.

Reference

Wernand, M. R., Hommersom, A. and van der Woerd, H. J.: [MERIS-based ocean colour classification with the discrete Forel–Ule scale](#), Ocean Sci., 9, 477-487, 2013

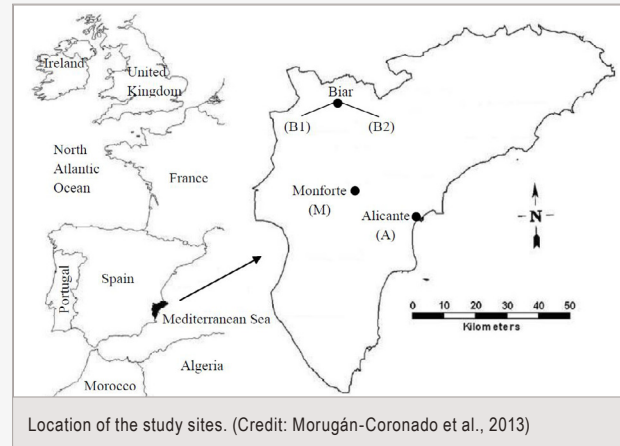
Solid Earth (SE)

Application of soil quality indices to assess the status of agricultural soils irrigated with treated wastewaters

In this work two soil quality indices were used to evaluate the effects of irrigation with treated wastewater in soils. The indices were developed studying different soil properties in undisturbed soils in south-east Spain, and the relationships between soil parameters were established using multiple linear regressions.

Reference

Morugán-Coronado, A., et al.: [Application of soil quality indices to assess the status of agricultural soils irrigated with treated wastewaters](#), *Solid Earth*, 4, 119-127, 2013



The Cryosphere (TC)

Ice-shelf buttressing and the stability of marine ice sheets

Ice-shelf buttressing and the stability of marine-type ice sheets are investigated numerically. Buttressing effects are analysed for a situation where a stable grounding line is located on a bed sloping upwards in the direction of flow.

Reference

Gudmundsson, G. H.: [Ice-shelf buttressing and the stability of marine ice sheets](#), *The Cryosphere*, 7, 647-655, 2013

Mechanisms causing reduced Arctic sea ice loss in a coupled climate model

The fully coupled climate model HadGEM1 produces one of the most accurate simulations of the historical record of Arctic sea ice seen in the IPCC AR4 multi-model ensemble. In this study, the researchers examine projections of sea ice decline out to 2030, produced by two ensembles of HadGEM1 with natural and anthropogenic forcings included.

Reference

West, A. E., Keen, A. B., and Hewitt, H. T.: [Mechanisms causing reduced Arctic sea ice loss in a coupled climate model](#), *The Cryosphere*, 7, 555-567, 2013

Estimating the Greenland ice sheet surface mass balance contribution to future sea level rise using the regional atmospheric climate model MAR

To estimate the sea level rise originating from changes in surface mass balance of the Greenland ice sheet, we present 21st century climate projections obtained with the regional climate model MAR (Modèle Atmosphérique Régional), forced by output of three CMIP5 (Coupled Model Intercomparison Project Phase 5) general circulation models.

Reference

Fettweis, X., et al.: [Estimating the Greenland ice sheet surface mass balance contribution to future sea level rise using the regional atmospheric climate model MAR](#), *The Cryosphere*, 7, 469-489, 2013

Surface undulations of Antarctic ice streams tightly controlled by bedrock topography

In this work researchers use recently acquired airborne radar data for the Rutford Ice Stream and Evans Ice Stream, and show that the surface response of fast-flowing ice is highly sensitive to bedrock irregularities with wavelengths of several ice thicknesses.

Reference

De Rydt, J. et al.: [Surface undulations of Antarctic ice streams tightly controlled by bedrock topography](#), *The Cryosphere*, 7, 407-417, 2013